

# TLBO-Based Optimal Speed Controller Design for Induction Motors Using Fuzzy Sliding Mode Controller

Alireza Alfi

Faculty of Electrical and Robotic Engineering, Shahrood University of Technology, Shahrood, Iran  
36199-95161, a\_alfi@shahroodut.ac.ir

**Abstract—** In this paper, Teaching-Learning-Based Optimization (TLBO) algorithm is employed for controlling the speed of induction motors using fuzzy sliding mode controller. The proposed control scheme formulates the design of the controller as an optimization problem. First, a sliding mode speed controller with an integral switching surface is designed, in which the acceleration information for speed control is not required. In this case, the upper bound of the lumped uncertainties including the parameter uncertainties and the load disturbance must be available. The importance of this parameter on the system performance is illustrated. Then, the fuzzy sliding mode speed controller is designed to estimate the upper bound of the lumped uncertainties. Finally, TLBO algorithm is adopted to determine the optimal upper bound of the uncertainty. Simulation results are given to demonstrate the superiority of the proposed controller in comparison with the proportional-integrator, traditional sliding mode controller, fuzzy sliding mode controller and adaptive fuzzy sliding mode controller.

**Keywords—** Induction motor, Sliding mode control, Teaching-learning-based optimization, Fuzzy control.

## I. INTRODUCTION

Variable speed drives for induction motor need both wide operating range of speed and fast torque response in the presence of disturbances and uncertainties leading to more advanced control approaches to meet the real demand. Indeed, in any control problem formulation, there exists difference between the real system and the mathematical model developed for the controller design, so-called model mismatch. The model mismatch may be due to un-modeled dynamics, perturbation in system parameters or approximation of the nonlinear system behavior by a linear model. The designer must ensure that the resultant controller has the ability to produce required performance levels against model mismatch. This has led to an intense interest in the development of robust control approaches.

Sliding Mode Controller (SMC) is one of the outstanding nonlinear controllers used to present a methodical solution for two main significant controllers' challenges, namely stability and robustness [1,2]. From this perspective, SMC in AC-Drive systems has drawn considerable attention in recent years [3-21]. This is because of the main advantages of this strategy including non-sensitivity to parameters variation, independence of external disturbances and quick response. In [22], SMC-based adaptive input-output linearizing control for induction motor drives was proposed. In this case, the motor flux amplitude and speed are separately controlled by SMCs with variable switching gains. The SMC with rotor flux estimation for induction motor drives was designed where rotor flux was estimated using a sliding mode observer [23,24]. In [25], the motion synchronization problem in dual spindle servo systems using a continuous time SMC was studied. In [26], a digital signal processor-based cross-coupled intelligent complementary SMC system was designed to implement synchronous control of a dual linear motor servo system. In [27], the speed synchronization of multiple induction motors using SMC law based on adjacent cross-coupling control structure was reported. In [28], a hybrid control system using a recurrent fuzzy neural network to control a linear induction motor servo drive was introduced. In [29], a new approach to indirect vector control of induction motors using fuzzy sliding mode was presented. In [30], the development of a decoupling mechanism and a speed control scheme based on sliding mode control theory for a direct rotor field oriented induction motors were focused.

The SMC design consists of two phases namely the hitting phase and the sliding phase. Before the system reaches the switching surface (hitting phase), the control directs the system towards the desired surface. When all the states of the controlled system lie within the plane, the sliding-mode occurs. In SMC, the dynamical behavior of the system is determined based on the switching surface

which is independent of the uncertainties and external disturbances. The control law with sliding mode surface is designed such that the state moves to the sliding mode surface in a finite time and stays there forever.

For control systems such as AC motor drive systems, switching frequency restriction causes the system states do not remain on the switching surface and oscillate around it, which is called chattering. This phenomenon is unfavorable, since the control effort increases and it triggers the high-frequency dynamics (un-modeled dynamics) of the system. Consequently, we address this problem, although this topic has been covered in the literature [31-33].

In order to reduce the chattering, different control methods have been devoted which can be classified into two categories: the boundary layer saturation and the estimated uncertainties methods. In boundary layer saturation method, the basic idea is the discontinuous method replacement by saturation (linear) method with small neighborhood of the switching surface. This replacement caused to increase the error performance against with the considerable chattering reduction. Research on estimated uncertainty to reduce the chattering is also significantly growing as their applications such as the applications of fuzzy logic on estimated uncertainty method. In [3], a Proportional-Integrator (PI) controller in the core of SMC was proposed to reduce the chattering. However, using the PI controller conduces to decreasing the speed of SMC. Hence, we have not utilized one of the important advantages of the SMCs, i.e. fast response. In [4], sliding mode speed controller was introduced with an integral switching surface in which the acceleration information for speed control is not required. In this reference, to solve the problem of the chattering, a continuous function was used instead of a *Sign* function in control signal. But, when designing this controller, the upper bound of uncertainties must be available. These uncertainties include the load torque and the mechanical parameters variation of the system that they are difficult to measure in practice. Thus, it is difficult to determine the upper bound of uncertainties. This parameter is the coefficient for the *Sign* function or continuous function and plays a key role for the chattering phenomenon. In [4], neglecting all uncertainties except the load torque, an adaptive algorithm was introduced to calculate the torque. This does not lead to appropriate response and the step response has a large overshoot. To solve this problem, in [6], Fuzzy SMC (FSMC) using adaptive tuning technique was designed.

Motivated by aforementioned discussions, based on [4], a sliding mode speed controller is designed using a different method to determine the upper bound of the uncertainties. Here, the upper bound is estimated by a fuzzy inference system. To optimize the estimated value, a novel Optimal Fuzzy Sliding Mode Controller (OFSMC) is introduced. In the core of OFSMC, Teaching-Learning-Based Optimization (TLBO) algorithm, which is a novel

population-based optimization technique, is employed. In TLBO, a group of learners is considered as population whereas different design variables are assumed as different subjects offered to the learners and learners' result is analogous to the fitness value of the optimization problem. In the entire population the best solution is considered as the teacher. In [34], the preferences of TLBO have been reported with other optimization methods, such as Genetic Algorithm (GA), Particle Swarm Optimization (PSO), Artificial Bee Colony (ABC), Ant Colony Optimization (ACO) and Harmony Search (HS). Unlike other optimization techniques, TLBO does not require any algorithm parameters to be tuned, thus making the implementation of TLBO simpler. In order to show the effectiveness of the OFSMC, its performance is compared with other control strategies including the conventional PI, SMC, FSMC and AFSMC [35]. Simulation results confirm that the performance of OFSMC is better than the others with respect to parameter variations and external disturbance. In addition, the proposed controller is working well in different possible situations under load and speed variations with minimal chattering.

The organization of this paper is as follows. First, the system description is explained. Then, the speed SMC and FSMC are represented and TLBO is briefly introduced as well. Afterward, the proposed OFSMC is given in detail. Finally, simulation results and conclusions are provided [35].

## II. SYSTEM DESCRIPTION

The electromagnetic model of three-phase induction motor, star connection and squirrel cage in synchronous reference frame is as follows [4]:

$$\begin{aligned} \frac{di_{ds}}{dt} = & -\left(\frac{R_s}{L_\delta} + \frac{R_r L_m^2}{L_\delta L_r^2}\right) i_{ds} + \omega_e i_{qs} \\ & - \frac{R_r L_m}{L_r^2 L_\delta} \Psi_{dr} + \frac{\omega_r L_m}{L_r L_\delta} \Psi_{qr} \\ & + \frac{1}{L_\delta} v_{ds} \end{aligned} \quad (1)$$

$$\begin{aligned} \frac{di_{qs}}{dt} = & -\omega_e i_{ds} - \left(\frac{R_s}{L_\delta} + \frac{R_r L_m^2}{L_\delta L_r^2}\right) i_{qs} \\ & - \frac{\omega_r L_m}{L_r L_\delta} \Psi_{dr} + \frac{R_r L_m}{L_r^2 L_\delta} \Psi_{qr} \\ & + \frac{1}{L_\delta} v_{ds} \end{aligned} \quad (2)$$

$$\begin{aligned} \frac{d\Psi_{dr}}{dt} = & \frac{R_r L_m}{L_r} i_{ds} - \frac{R_r}{L_r} \Psi_{dr} \\ & + (\omega_e - \omega_r) \Psi_{qr} \end{aligned} \quad (3)$$

$$\frac{d\Psi_{qr}}{dt} = \frac{R_r L_m}{L_r} i_{qs} - (\omega_e - \omega_r) \Psi_{dr} - \frac{R_r}{L_r} \Psi_{qr} \quad (4)$$

where  $i, \Psi, v, R$  and  $L$  represent the current, flux linkage, voltage, resistance and inductance, respectively, the indices  $s$  and  $r$  denote the stator and rotor, respectively,  $q$  and  $d$  are the components in two-axis reference frame,  $\omega_r$  and  $\omega_e$  designate the angular speed for rotor and synchronously rotating speed, respectively,  $L_m$  and  $L_\delta$  stand for the mutual and leakage inductances, ( $L_\delta = L_s - \frac{L_m^2}{L_r}$ ).

The torque generated by the motor  $T_e$  and the corresponding mechanical relationships are given by

$$T_e = \frac{3PL_m}{4L_r} (\Psi_{dr} i_{qs} - \Psi_{qr} i_{ds}) \quad (5)$$

$$J \dot{\omega}_m(t) + B\omega_m + T_L = T_e \quad (6)$$

where  $T_L$  is the load torque,  $J$  is the moment of inertia,  $B$  is the coefficient of viscous friction, and  $P$  is the number of pole pairs.

Using indirect vector control, in the ideal case, it can be obtained [10]

$$\Psi_{qr} = \frac{d\Psi_{qr}}{dt} = 0 \quad (7)$$

$$\Psi_{dr} = L_m i_{ds}^* \quad (8)$$

$$T_e = K_t i_{qs} \quad (9)$$

$$K_t = \frac{3p}{4} \left( \frac{L_m^2}{L_r} \right) i_{ds}^* \quad (10)$$

$$\omega_e - \omega_r = \frac{R_r i_{qs}^*}{L_r i_{ds}^*} \quad (11)$$

where  $i_{qs}^*$  and  $i_{ds}^*$  are the torque generating and the flux generating commands, respectively.

### III. SLIDING MODE SPEED CONTROLLER

#### A. Nominal model

Considering the zero disturbance load torque with together the nominal parameters of the motor, the mechanical equation can be represented as

$$\dot{\omega}_m(t) = -\frac{B_n}{J_n} \omega_m + \frac{K_t}{J_n} i_{qs}^*(t) = a_n \omega_m + b_n u(t) \quad (12)$$

where  $a_n = -\frac{B_n}{J_n}$ ,  $b_n = \frac{K_t}{J_n}$ ,  $u(t)$  is the control effort, and the subscript “ $n$ ” denotes the nominal value.

Based on the feedback linearization theory [36], a nominal speed controller is designed as

$$u_n(t) = -b_n^{-1} a_n \omega_m + b_n^{-1} [\dot{\omega}_m^* - k_v e] \quad (13)$$

where

$$e(t) = \omega_m(t) - \omega_m^* \quad (14)$$

in which  $\omega_m^*$  is the speed command.

Substituting (13) into (12), the dynamic of speed error is

$$\dot{e} + k_v e = 0 \quad (15)$$

From (15), the desired speed error dynamic can be achieved by adjusting the parameter  $k_v$ . The above nominal controller cannot guarantee the stability and robust performance of the system simultaneously in presence of load torque disturbance and uncertainties including the mechanical parameter ( $J, B$ ). This problem is investigated in the next subsection.

#### B. Uncertain model

Considering the external load torque and variations existed in parameters  $J_n$  and  $B_n$ , the perturbed mechanical equation given in (6) can be expressed as

$$\dot{\omega}_m(t) = (a_n + \Delta a) \omega_m(t) + (b_n + \Delta b) u(t) + d_n T_L \quad (16)$$

where  $d_n = -\frac{1}{J_n}$ , and  $\Delta a$  and  $\Delta b$  are the parameters uncertainties related to  $a$  and  $b$ , respectively.

The above equation can be rewritten as

$$\dot{\omega}_m(t) = a_n \omega_m(t) + b_n [u(t) + \Delta(t)] \quad (17)$$

where  $\Delta(t)$  denotes the lumped uncertainty, which is assumed to be bounded, as

$$\Delta(t) = \frac{\Delta a}{b_n} \omega_m(t) + \frac{\Delta b}{b_n} u(t) + \frac{d_n}{b_n} T_L \quad (18)$$

Taking the time derivative of (14) and substituting (17) into it, the following error dynamic of speed can be obtained.

$$\dot{e}(t) = a_n e(t) + b_n [\dot{u}(t) + \Delta(t)] \quad (19)$$

and

$$\dot{u}(t) = \dot{u}(t) + \frac{a_n}{b_n} \omega_m^* \quad (20)$$

In the following, the switching surface for the system is introduced.

#### C. Design of switching surface

Consider the switching surface for speed control system [4]

$$S(t) = e(t) - e(0) - \int_0^t (a_n + b_n k_v) e(\tau) d\tau \quad (21)$$

where  $k_v$  is the linear feedback gain.

It is apparent that to calculate  $S$ , the speed error signal is only required. If one can hold the state trajectories of the system (19) on switching surface given in (21), i.e.  $S(t) = \dot{S}(t) = 0$ , then the dynamical behavior of speed control system would not be sensitive with respect to the uncertainties and the external load torque. As a result, we have

$$\dot{e}(t) = (a_n + b_n k_v) e(t) \quad (22)$$

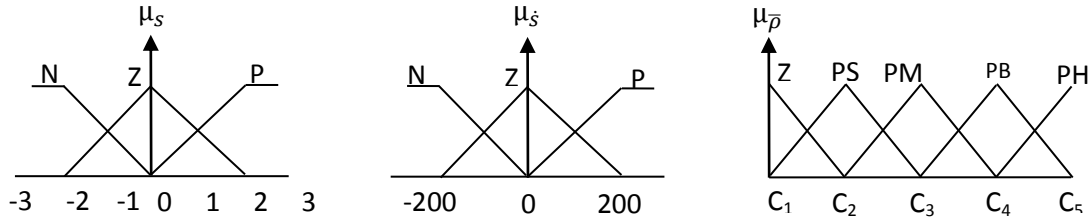


Fig. 1. Membership functions of fuzzy sets [35].

It is clearly obvious that if the poles of above equation are in the open left half-plane, then the speed error converges exponentially to zero.

#### D. Design of speed controller

According to the switching surfaces given in (21), it is desirable to obtain a control law that can satisfy the hitting condition and guarantees the existence of the SMC. To this end, the following speed controller is proposed.

$$\bar{u}(t) = k_v e(t) - \rho \operatorname{sgn}(S(t)), \quad \rho > 0 \quad (23)$$

where  $\operatorname{sgn}(\cdot)$  is a sign function and  $\rho$  is the upper bound of lumped uncertainties, i.e.

$$|\Delta(t)| \leq \rho \quad (24)$$

Substituting (23) in (20), the torque-generating current command or the output of speed controller ( $i_{qs}^*$ ) is obtained. Taking the time derivative of the Lyapunov function  $V(t) = \frac{1}{2} S^2(t)$ , and using (19) and (23), we have

$$\begin{aligned} S(t)\dot{S}(t) &= S(t) \{ \dot{e}(t) - (a_n + b_n k_v) e(t) \} \\ &= S(t) \{ a_n e(t) + b_n \bar{u}(t) + b_n \Delta(t) - a_n e(t) - b_n k_v e(t) \} \\ &= S(t) \{ b_n k_v e(t) - b_n \rho \operatorname{sgn}(S(t)) + b_n \Delta(t) - b_n k_v e(t) \} \\ &= b_n (\Delta(t) S(t) - \rho |S(t)|) \\ &\leq -b_n |S(t)| (\rho - |\Delta(t)|) \\ &\leq 0 \end{aligned}$$

Therefore, the existence of sliding mode condition

$$S(t)\dot{S}(t) \leq 0 \quad (25)$$

is satisfied. The problem here is the determination of  $\rho$ . From (18), it can be seen that this parameter is difficult to obtain. Referring to (23),  $\rho$  is the coefficient of  $\operatorname{Sign}$  function meaning this parameter can affect on chattering. On the other hand, we will show that when this parameter becomes irrationally large, it leads to chattering, even if a continuous function is used as an alternative of  $\operatorname{Sign}$  function in control signal. The next section introduces a fuzzy inference mechanism to estimate the upper bound of the lumped uncertainties  $\rho$ .

*Remark 1:* To reduce the chattering phenomenon, the  $\operatorname{Sign}$  function in speed controller can be replaced by the following smooth function.

$$g(s) = \frac{1 - e^{-\tau s}}{1 + e^{-\tau s}}, \quad \tau > 1 \quad (26)$$

#### IV. SPEED FSMC

In this section, the fuzzy rules are provided. Let define a new parameter  $\bar{\rho}$  as an estimated upper bound of the lumped uncertainties by the fuzzy mechanism. Substituting  $\bar{\rho}$  in (23) yields

$$\bar{u}(t) = k_v e(t) - \bar{\rho} \operatorname{sgn}(S(t)), \quad \bar{\rho} > 0 \quad (27)$$

We will have a new prospect towards  $\bar{\rho}$  aside from the uncertainties. Eq. (27) shows that  $\bar{\rho}$  is the control gain applied to the system to direct the system states to the switching surface. In other words, whenever  $S$  is positive, Eq. (27) can be written as

$$\bar{u}(t) = k_v e(t) - \bar{\rho} \quad (28)$$

We also know that the above signal is the torque generating current command so reducing this signal will decrease the produced torque. This causes the parameter  $S$  goes to zero. If  $S$  is negative, we get

$$\bar{u}(t) = k_v e(t) + \bar{\rho} \quad (29)$$

Therefore, the control effort and consequently speed increases. Using (28) and (29), we realize that in both above cases  $\bar{\rho}$  is the quantity of control effort applied to the system. We can apply this fact in how to determine  $\bar{\rho}$ . It is noticeable that the states of the system are farther from the sliding surface, the more control gain is required to be implemented to the system. If the value of parameter  $\bar{\rho}$  is correctly chosen such that the states of system go towards the switching surface from any arbitrary initial point, then it can be inferred that  $\bar{\rho}$  is the upper bound of the lumped uncertainties. Based on above explanation to determine  $\bar{\rho}$ , a fuzzy inference mechanism is proposed. This mechanism estimates  $\bar{\rho}$  according to  $S$  and  $\dot{S}$  as the inputs of the fuzzy system. The associated fuzzy sets are considered as N: Negative, Z: Zero, P: Positive, PS: Positive Small, PH: Positive Huge, PB: Positive Big, PM: Positive Medium. The membership functions corresponding to  $S, \dot{S}$  and  $\bar{\rho}$  are depicted in Fig. 1 [35]. The fuzzy rules are also defined as follows:

*Rule 1:* IF  $\{(S \text{ is } P \text{ and } \dot{S} \text{ is } P) \text{ or } (S \text{ is } N \text{ and } \dot{S} \text{ is } N)\}$  THEN  $\rho$  is PH

*Rule 2:* IF  $\{(S \text{ is } P \text{ and } \dot{S} \text{ is } Z) \text{ or } (S \text{ is } N \text{ and } \dot{S} \text{ is } Z)\}$  THEN  $\rho$  is PB

*Rule 3:* IF  $\{(S \text{ is } P \text{ and } \dot{S} \text{ is } N) \text{ or } (S \text{ is } N \text{ and } \dot{S} \text{ is } P)\}$  THEN  $\rho$  is PM

*Rule 4:* IF  $\{(S \text{ is } Z \text{ and } \dot{S} \text{ is } P) \text{ or } (S \text{ is } Z \text{ and } \dot{S} \text{ is } N)\}$  THEN  $\rho$  is PS

Rule 5: IF  $\{(S \text{ is } Z \text{ and } \dot{S} \text{ is } Z)\}$  THEN  $\rho$  is Z

Using the center of mass defuzzification method, the crisp output  $\bar{\rho}$  can be obtained as

$$\bar{\rho} = \frac{\sum_{i=1}^5 \mu_i c_i}{\sum_{i=1}^5 \mu_i} = \frac{[c_1 \dots c_5] \begin{bmatrix} \mu_1 \\ \vdots \\ \mu_5 \end{bmatrix}}{\sum_{i=1}^5 \mu_i} = C^T \mu \quad (30)$$

where  $\mu_i, i = 1, \dots, 5$  is the degree of membership of  $i$  rule and  $C = [C_1 \dots C_5]$  are the centers of output membership functions which are the adjustable parameters.

Now the problem is how to determine the vector  $C$  properly. It means that, there exists an optimal value for  $\bar{\rho}$ . In the simulations, we show that the improper value  $C$  causes  $\bar{\rho}$  not to be estimated appropriately. Consequently, in order to estimate the optimum upper bound of the lumped uncertainties, it is better to determine this vector based upon the operating conditions of the motor and also to be changed in various conditions. To handle this problem, the proposed method formulates the design of FSMC as an optimization problem using TLBO to find the optimal vector values of  $C$ . In the next section, we explain the proposed OFSMC in detail.

Remark 2: The proposed control method can be adopted both in position and speed control drives. The position control system is thoroughly similar to the speed control system. The only difference appears to be of the feedback signals, in that the speed controller must provide the current command signal  $i_{qs}^*$  according to them. The switching surface for position control system is defined as

$$S(t) = \dot{e}_\theta - (a_n + b_n k_v) e_\theta(t) \quad (31)$$

where

$$e_\theta(t) = \theta_m(t) - \theta_m^* \quad (32)$$

and  $\theta_m^*$  is the position command.

In the position control system, we have

$$\omega_m^* = \dot{\theta}_m^* \quad (33)$$

Considering  $S=0$  in (31) in this case, it yields

$$\dot{e}_\theta = (a_n + b_n k_v) e_\theta(t) \quad (34)$$

It is straightforward to see that if the poles of the system given in Eq. (34) are in the open left half-plane, then the position errors converge exponentially to zero.

### V. TLBO ALGORITHM

In this section, the TLBO algorithm is described. Then, TLBO is employed into the problem in hand. TLBO algorithm, originally developed by Rao et al. [34], is a population-based optimization algorithm. In TLBO algorithm a population of solutions is utilized to proceed to the global solution. To this end, in TLBO algorithm, a group of learners is chosen as population and different

design variables are considered as different subjects offered to the learners. Learners' result is similar to the 'fitness' value of the optimization problem. In the whole population, the best solution is considered as the teacher.

The two elementary components of this algorithm are teacher and learners. Based on two basic modes of the learning, through teacher (known as teacher phase) and interacting with the other learners (known as learner phase), the procedure of TLBO is divided into two parts, the Teacher and the Learner phases. The first part of the algorithm is teacher phase where learners learn through the teacher. During this phase, a teacher attempts to increase the mean result of the class in the subject taught by him or her depending on his or her capability. At any iteration  $i$ , assume that there are 'm' number of subjects (i.e. design variables), 'n' number of learners (i.e. population size,  $k=1,2,\dots,n$ ). Consider  $M_i$  be the mean and  $T_i$  be the teacher at any iteration  $i$ .  $T_i$  will try to enhance existing mean  $M_i$  towards it so the new mean will be  $T_i$  designated as  $M_{new}$ . The solution is updated according to the difference between the existing and the new mean given by

$$Difference\_Mean_i = r_i (Mean_{new} - T_F M_i) \quad (35)$$

where  $T_F$  is the teaching factor which decides the value of mean to be changed, and  $r_i$  is the random number in the range  $[0, 1]$ . The teaching factor  $T_F$  is generated randomly during the algorithm in the range of 1-2, in which 1 corresponds to no increase in the knowledge level and 2 refers to complete transfer of knowledge. The value of  $T_F$  is randomly opted with equal probability as

$$T_F = round[1 + rand(0,1)\{1 - 2\}] \quad (36)$$

Using Eq. (35), the existing solution is updated as

$$X_{new,i} = X_{old,i} + Difference\_Mean_i \quad (37)$$

In the learner phase, the learners can enhance their knowledge via interaction among themselves randomly. A learner learns new things if the other learner has more knowledge than him or her. The learning phenomenon of this phase at any iteration  $i$  for two different learners  $X_i$  and  $X_j$  where  $i \neq j$  are given by

$$X_{new,i} = X_{old,i} + r_j (X_i - X_j), \quad \text{if } f(X_i) < f(X_j) \quad (38)$$

$$X_{new,i} = X_{old,i} + r_j (X_j - X_i), \quad \text{if } f(X_j) < f(X_i) \quad (39)$$

where  $f(X) = \frac{1}{\sigma\sqrt{2\pi}} e^{-\frac{(x-\mu)^2}{2\sigma^2}}$  is the normal distribution

in which  $\sigma^2$  is the variance and  $\mu$  is the mean value.



KW. The parameters of this motor are listed in Table 1 [4]. The current controller is also a conventional PI controller and the related output is the voltage commands. In order to realize the commands, the space vector pulse width modulation method is employed with switching frequency of 4KHZ. Moreover,  $\tau$  is equal to 5. In addition, the block diagram of Fig. 2 is thoroughly simulated in the speed control. Here, the population size and the maximum number of generations are taken as 10 and 100, respectively, for all the test system under consideration. In all simulations, TLBO algorithm is run for 50 times independently and the best result is listed. The obtained parameters of vector  $C$  via TLBO algorithm are [1.86 9.47 26.05 1.15 5.68].

To show the feasibility of the proposed OFSMC, the results are compared with those obtained from PI controller, SMC, FSMC, and AFSMC. Appendix A gives more details about AFSMC. To this end, simulation results are performed for two cases in starting and loading conditions: with uncertainties and without uncertainties, whereas disturbance is considered both in two cases. The uncertainties being taken into account are the variation in moment of inertia and damping coefficient as  $J = 4J_n$  and  $B = 4B_n$ . The external torque  $T_L$  is also considered as a step function with amplitude 2N.m. Both the external torque and speed step command is simultaneously applied to the motor at  $t=0.5 \text{ sec}$ . To compare the behavior of the

speed controllers, the external torque is used at the starting moment.

Figs. 3-16 depict the simulation results. Figs. 3-7 illustrate the step response for different controller. In these Figs., two principal responses, i.e. the speed  $\omega_m$  and the controller's output  $i_{qs}^*$ , are shown. The speed response represents the ability of the controller and the controller's output indicates the control effort. Among all current controllers,  $i_{qs}^*$  is restricted to 15A. Fig. 3 exhibits the PI controller response. In addition, the proportional  $K_p$  and integral  $K_i$  gains of the PI controller are chosen 0.2 and 0.02, respectively. It can be seen that the PI controller has a slow response and improper damped step response due to the parameter variations.

Fig. 4 shows the SMC response. Here, a constant value is considered for the upper bound of the lumped uncertainty. It is noticeable that the upper bound of the lumped uncertainty is generally unknown and depends on the load torque. Referring to Fig. 4.b, it can be obvious that while the system is without uncertainties (Fig. 4.b) the value set for  $\rho$  causes chattering phenomenon in the current response.

The performance of FSMC is also presented in Fig. 5. In this case, a fuzzy interface mechanism is used to estimate the upper bound of uncertainties. Here, the parameters of

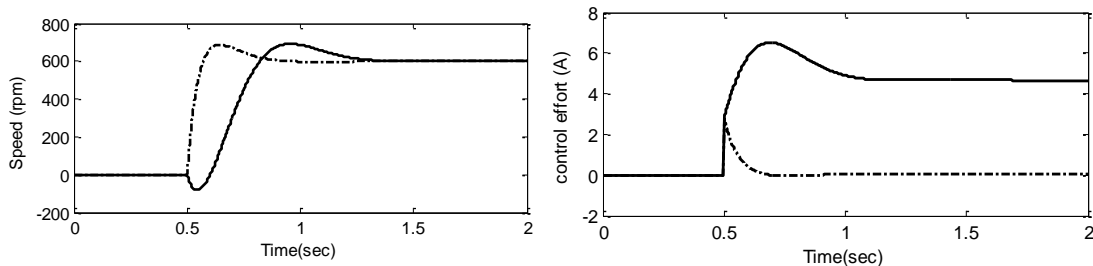


Fig. 3. Step response of conventional PI controller without (-) and with uncertainties (-).

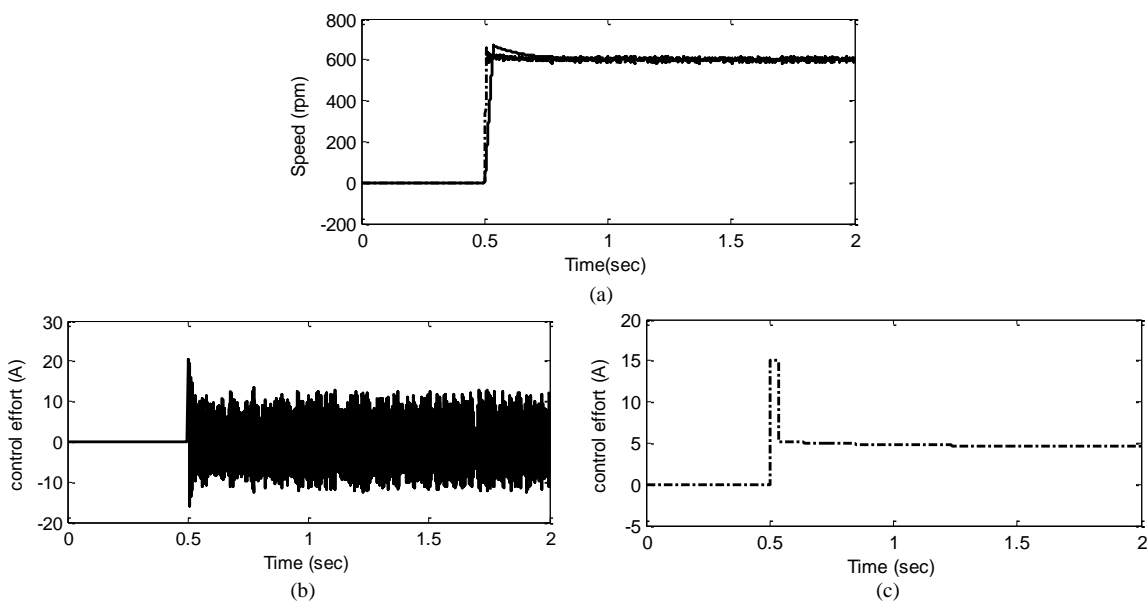


Fig. 4. Step response of SMC without (-) and with uncertainties (-).

vector  $C$  is chosen [0 1 2 3 4]. Without considering uncertainties, the responses do not have any problem. However, because  $C$  is not accurate,  $\rho$  is not estimated properly and this leads to a steady-state error (about 100 rpm) in speed response as shown in Fig. 5. In Figs. 6 and 7, the centers of membership functions are computed by adaptive algorithm and TLBO, respectively. The initial value for  $C$  is zero. Referring to Fig. 7, it is apparent that the TLBO algorithm can appropriately determine the optimum value of  $C$  such that the responses for both cases (with and without uncertainties) are desirable. It is clearly inferred that the chattering phenomenon does not exist in the current response. Figs. 8-11 exhibit the lumped uncertainty  $\Delta(t)$  and the upper bound of uncertainties  $\rho$  for the aforementioned controllers. In SMC,  $\rho$  is set to 20. These figures reveal that the responses of OFSMC are satisfactory. From Fig. 8b, it can be seen that the fuzzy algorithm is unable to estimate the proper upper bound of uncertainties. Figs. 9 and 10 correspond to the AFSMC and OFSMC, respectively. From these figures, it is apparent that the performance of OFSMC is better than the AFSMC regarding to estimating the upper bound for error. To further verify the performance of OFSMC, the results are illustrated for different operating points of motor. The obtained results including the speed response and the control effort are given in Figs. 12-16. In this case, the motor is rotating with a speed of 1000 rpm that the full load torque is applied. It is observed that the conventional PI controller does not have appropriate response. Furthermore, by applying load torque, the speed collapses instantaneously. The response for FSMC is not desirable as shown in Fig. 14. This discrepancy can be overcome by proper adjustment of the upper bound of uncertainties. Fig. 16 reflects the ability of OFSMC to estimate the proper upper bound of uncertainties to have a good response. It can be concluded that the proposed OFSMC is working well in different possible situations under load and speed variations.

## VIII. CONCLUSION

The main purpose of this paper was to propose a novel OFSMC design for controlling the speed of induction motor drives. In the core of the proposed controller, a fuzzy inference system was adopted to estimate the upper bound of the uncertainties. It was found that the improper choice of the centers of membership functions leads to steady-state error in speed response. To overcome this problem, TLBO algorithm was employed to optimize the centers of membership functions with respect to different operating conditions. According to the simulation results, the proposed OFSMC provided better results than PI, SMC, FSMC and AFSMC in different possible conditions under load and speed variations.

## APPENDIX

In the AFSMC, the parameters vector  $C$  are adjusted by the following adaptive law [37]

$$\dot{C} = \gamma b_n |S| \mu \quad (\text{A.1})$$

where  $\gamma$  is a positive constant.

It can be seen that to calculate each membership function center, the value for  $S$  and the value of membership degree of the corresponding rule are important. Let us define  $\bar{\rho}$  as an optimum value of error estimation. From (30), we have

$$\bar{\rho} = \tilde{C}^T \mu \quad (\text{A.2})$$

$\hat{C}$  is the optimum vector corresponding to  $\bar{\rho}$ . The error can be represented as

$$\tilde{C} = C - \hat{C} \quad (\text{A.3})$$

In order to analyze the closed-loop stability, the following Lyapunov function candidate is considered.

$$V = \frac{1}{2} \left( s^2 + \frac{1}{\gamma} \tilde{C}^T \tilde{C} \right) \quad (\text{A.4})$$

Taking the derivative of Eq. (A.4) with respect to time, it yields

$$\begin{aligned} \dot{V} &= s\dot{s} + \frac{1}{\gamma} \tilde{C}^T \dot{\tilde{C}} \\ &= s \left( [\dot{e}_\omega - (a_n + b_n k_v) e_\omega] + \frac{1}{\gamma} \tilde{C}^T \dot{\tilde{C}} \right) \\ &= s(a_n e + b_n \bar{u} + b_n \Delta - a_n e - b_n k_v e) + \frac{1}{\gamma} \tilde{C}^T \dot{\tilde{C}} \\ &= c(b_n k_v e - b_n \rho s g n(s) + b_n \Delta - b_n k_v e) + \frac{1}{\gamma} \tilde{C}^T \dot{\tilde{C}} \\ &\leq -b_n |s| (\rho - |\Delta|) + \frac{1}{\gamma} \tilde{C}^T \dot{\tilde{C}} \\ &= -b_n |s| (\bar{\rho} - |\Delta| + \rho - \bar{\rho}) + \frac{1}{\gamma} \tilde{C}^T \dot{\tilde{C}} \\ &= -b_n |s| (\bar{\rho} - |\Delta|) - b_n |s| \tilde{C}^T \mu + \frac{1}{\gamma} \tilde{C}^T \dot{\tilde{C}} \\ &= -b_n |s| (\bar{\rho} - |\Delta|) - \frac{1}{\gamma} \tilde{C}^T (\dot{\tilde{C}} - \gamma b_n |s| \mu) \end{aligned} \quad (\text{A.5})$$

Choosing the adaptive law given in Eq. (A.1), we obtain

$$\dot{V} = -b_n |s| (\bar{\rho} - |\Delta|) < 0 \quad (\text{A.6})$$

## ACKNOWLEDGMENT

This work was supported by a grant from The Shahrood University of Technology (No. 13040).

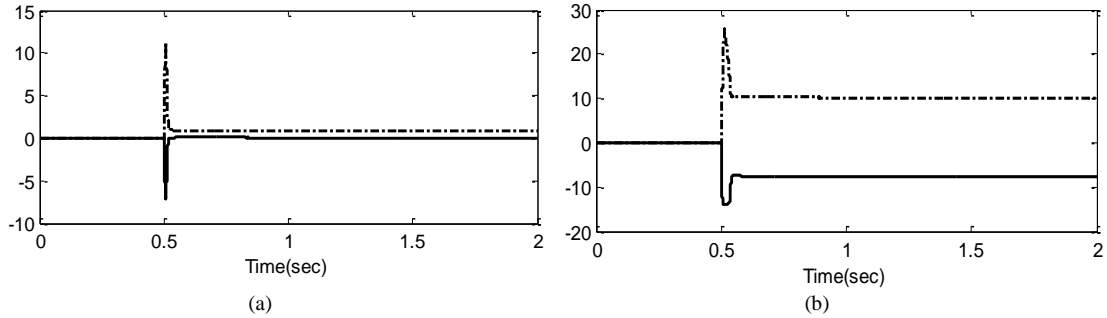


Fig. 11. Lumped uncertainty and upper bound of uncertainties using OFSMC (a) without uncertainties (b) with uncertainties.

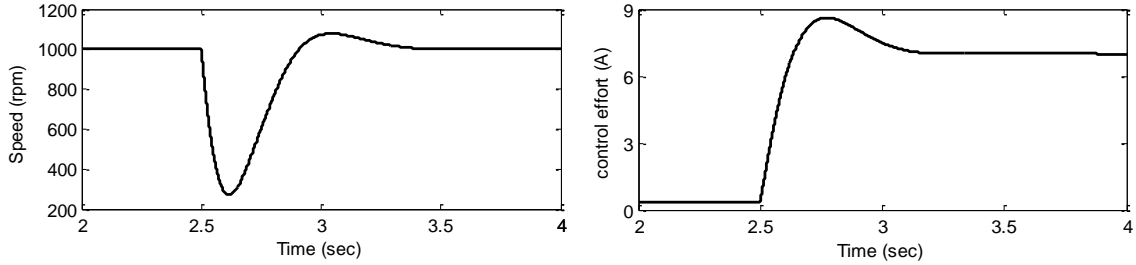


Fig. 12. Conventional PI response with variation in operating point.

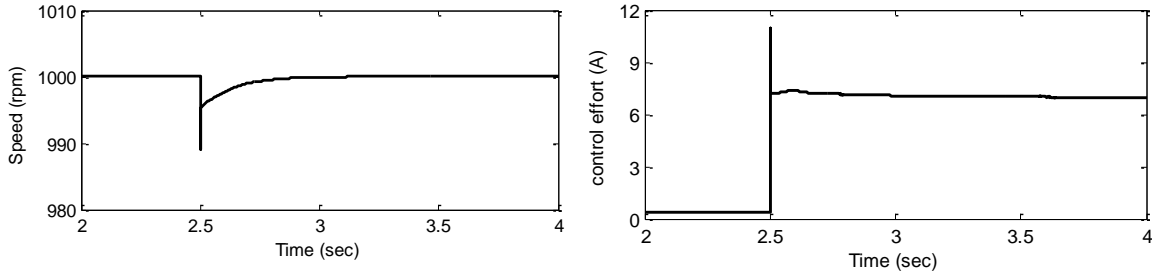


Fig. 13. SMC response with variation in operating point.

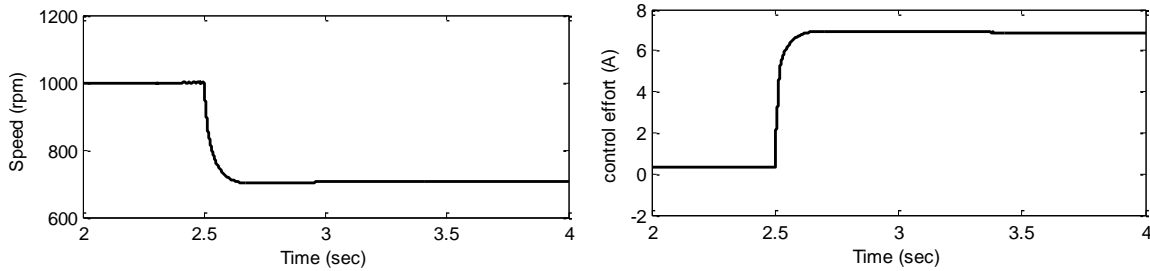


Fig. 14. FSMC with variation in operating point.

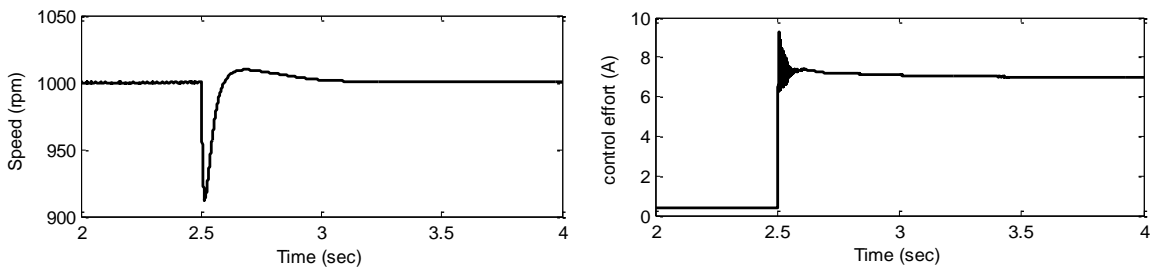


Fig. 15. AFSMC response with variation in operating point.

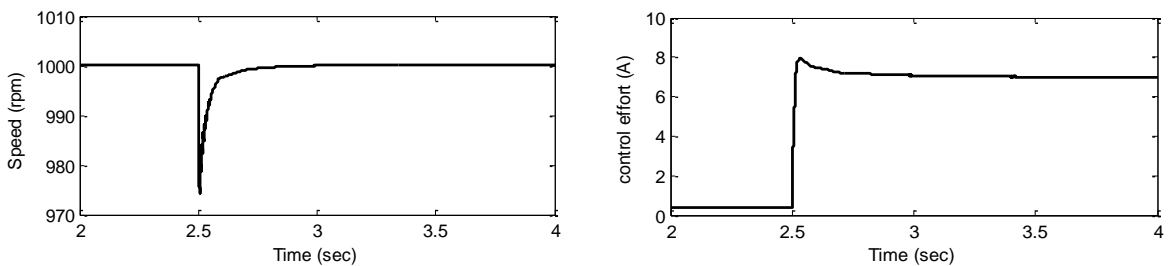


Fig. 16. OFSMC response with variation in operating point.

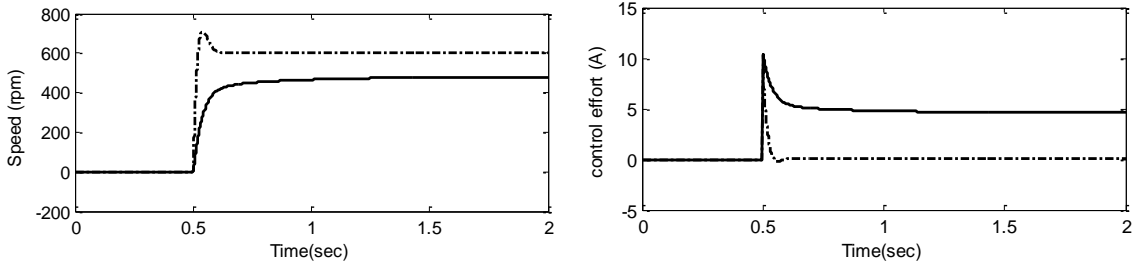


Fig. 5. Step response of FSMC without (-) and with uncertainties (-).

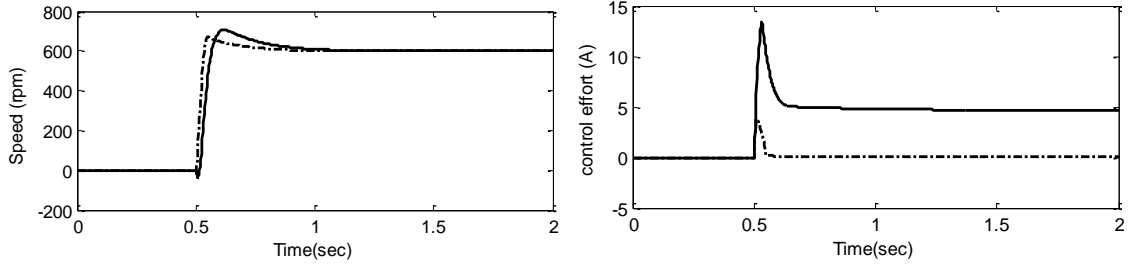


Fig. 6. Step response of AFSMC without (-) and with uncertainties (-).

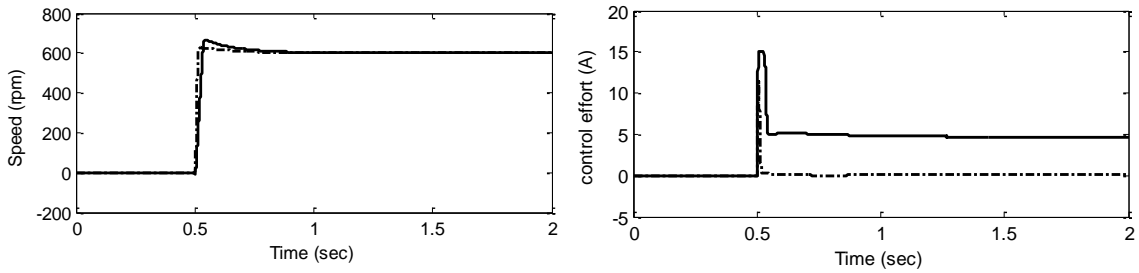


Fig. 7. Step response of OFSMC without (-) and with uncertainties (-).

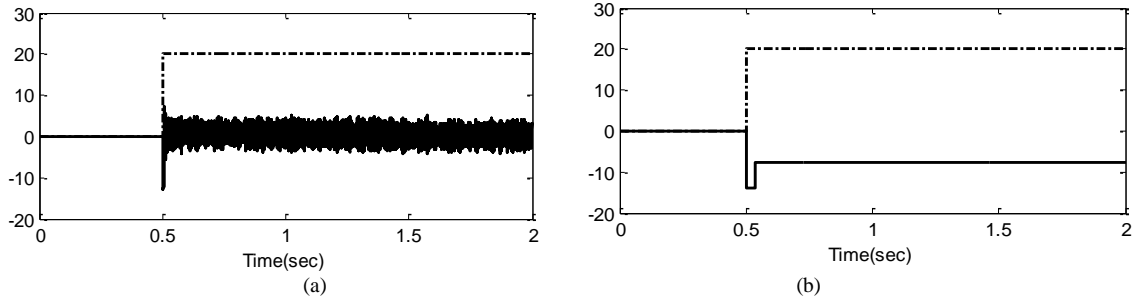


Fig. 8. Lumped uncertainty and upper bound of uncertainties using SMC (a) without uncertainties (b) with uncertainties.

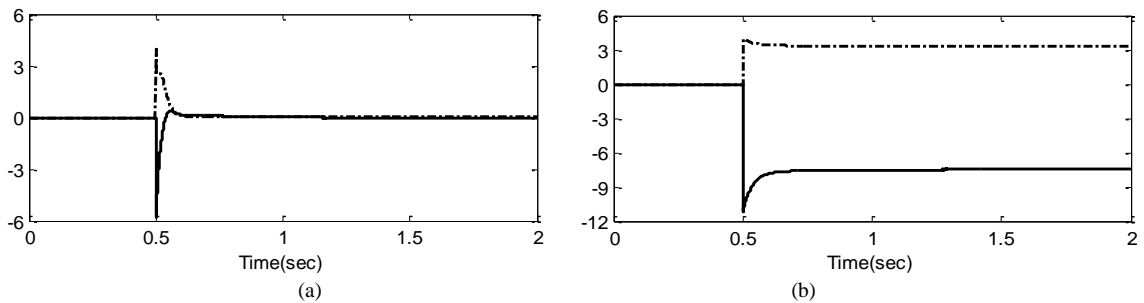


Fig. 9. Lumped uncertainty and upper bound of uncertainties using FSMC (a) without uncertainties (b) with uncertainties.

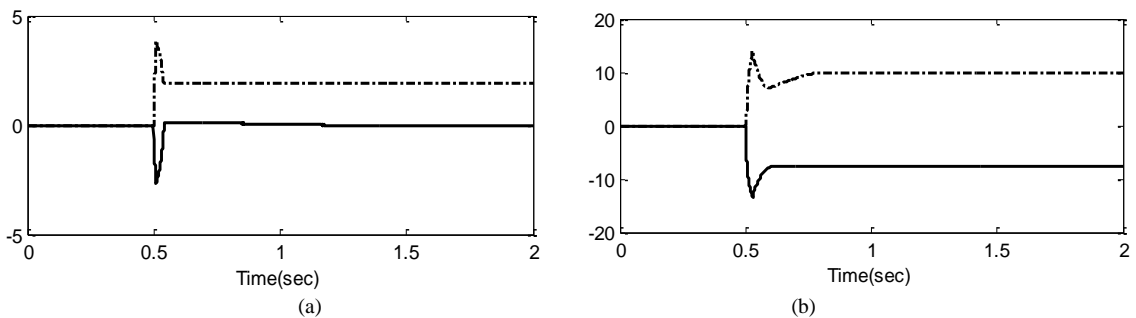


Fig. 10. Lumped uncertainty and upper bound of uncertainties using AFSMC (a) without uncertainties (b) with uncertainties.

## REFERENCES

- [1] Z. Al-Hamouza, H. Al-Duwaisha, N. Al-Musabi, Optimal design of a sliding mode AGC controller: Application to a nonlinear interconnected model, *Elect. Power Syst. Res.* 81 (2011) 1403–1409.
- [2] S. Meradia, K. Benmansourb, K. Herizia, M. Tadjinea, M.S. Boucherit, Sliding mode and fault tolerant control for multicellular converter four quadrants, *Elect. Power Syst. Res.* 95 (2013) 128–139.
- [3] E.Y.Y. Ho, P.C. Sen, Control dynamics of speed drive systems using sliding mode controller with integral compensation, *IEEE Trans. Ind. Appl.* 27 (1991) 883–892.
- [4] K.K. Shyu, H.S. Shieh, A new switching surface sliding-mode speed control for induction motor drive systems, *IEEE Trans. Power Electron.* 11 (1996) 660–667.
- [5] W.J. Wang, J.Y. Chen, Passivity-based sliding mode position control for induction motor drives, *IEEE Trans. Energy Convers.* 20 (2005) 1–10.
- [6] R.J. Wai, Fuzzy sliding-mode control using adaptive tuning technique, *IEEE Trans. Ind. Electron.* 54 (2007) 586–594.
- [7] T.O. Kowalska, M. Dybkowski, K. Szabat, Adaptive sliding-mode neuro-fuzzy control of the two-mass induction motor drive without mechanical sensors, *IEEE Trans. Ind. Electron.* 57 (2010) 553–564.
- [8] R.J. Wai, K.H. Su, Adaptive enhanced fuzzy sliding-mode control for electrical servo drive, *IEEE Trans. Ind. Electron.* 53 (2006) 569–580.
- [9] S. Ryvkin, R.S. Obermoeller, A. Steimel, Sliding-mode-based control for a three-level inverter drive, *IEEE Trans. Ind. Electron.* 55 (2008) 3828–3835.
- [10] B.K. Bose, *Power Electronics and AC Drives*, Prentice-Hall, 1986.
- [11] M.G. Aydeniz, I. Senol, A Luenberger-sliding mode observer with rotor time constant parameter estimation in induction motor drives, *Turk. J. Elec. Eng. & Comp. Sci.* 19 (2011) 901–1002.
- [12] G.J. Rubio, J.M. Cañedo, V.I. Utkin, A.G. Loukianov, Second order sliding mode block control of single-phase induction motors, *Robust Nonlinear Control*, DOI: 10.1002/rnc.2913 (2012)
- [13] Y. Feng, M. Zhou, X. Yu, Sliding-mode observer based flux estimation of induction motors, *Lecture Notes in Computer Science, Intelligent Robotics and Applications*, 7507 (2012) 530–539.
- [14] H. Benderradji, A. Benamor, L. Chrifi-Alaoui, P. Bussy, A. Makouf, Second order sliding mode induction motor control with a new Lyapunov approach, *Proceedings of the 9<sup>th</sup> International Multi-Conference on Systems, Signals and Devices*, pp. 1–6, 2012.
- [15] R.P. Vieira, C.C. Gastaldini, R.Z. Azzolin, H.A Grundling, Discrete-time sliding mode speed observer for sensorless control of induction motor drives, *IET Electr. Power Appl.* 6 (2012) 681–688.
- [16] A.Y. Alanis, E.N. Sanchez, A.G. Loukianov, M.A. Perez-Cisneros, Real-time discrete neural block control using sliding modes for electric induction motors, *IEEE Trans. Control Syst. Tech.* 18 (2010) 11–21.
- [17] T. Orłowska-Kowalska, M. Dybkowski, K. Szabat, Adaptive sliding-mode neuro-fuzzy control of the two-mass induction motor drive without mechanical sensors, *IEEE Trans. Ind. Electron.* 57 (2010) 553–564.
- [18] J.Y. Hung, W. Gao, J.C. Hung, variable structure control: a survey, *IEEE Trans. Ind. Electron.* 40 (1993) 2–22.
- [19] B. Veselic, B.P. Drzenovic, C. Milosavljevic, Improved discrete-time sliding-mode position control using Euler velocity estimation, *IEEE Trans. Ind. Electron.* 57 (2010) 3840–3847.
- [20] M. Comanescu, An induction-motor speed estimator based on integral sliding-mode current control, *IEEE Trans. Ind. Electron.* 56 (2009) 3414–3423.
- [21] C.C. Chan, H.Q. Wang, New scheme of sliding mode control for high performance induction motor drives,” *IEE Proc. Electric. Power Appl.* 143 (1996) 177–185.
- [22] T.G. Park, K.S. Lee, SMC based adaptive input-output linearizing control of induction motors, *IEE Proc. Control Theory Appl.* 145 (1998) 55–62.
- [23] A. Benchaib, A. Rachid, E. Audrezet, Sliding made input-output linearization and field orientation for real time control of induction motors, *IEEE Trans. Power Electr.* 14 (1999) 128–138.
- [24] A. Benchaib, A. Rachid, E. Audrezet, M. Tadjine, Real time sliding mode observer and control of an induction motor, *IEEE Trans. Ind. Electr.* 46 (1999) 128–138.
- [25] B. Sencer, T. Mori, E. Shamoto, Design and application of a sliding mode controller for accurate motion synchronization of dual servo systems, *Control Engineering Practice* 21 (2013) 1519–1530.
- [26] L. Faa-Jeng, C. Po-Huan, C. Chin-Sheng, L. Yu-Sheng, DSP-based cross-coupled synchronous control for dual linear motors via intelligent complementary sliding mode control, *IEEE Trans. Indust. Elec.* 59 (2012) 1061–1073.
- [27] D.Z. Zhao, C.W. Li, J. Ren, Speed synchronization of multiple induction motors with adjacent cross coupling control, *Proceedings of the 48<sup>th</sup> IEEE Conference on Decision and Control*, 2009, pp.6805–6810.
- [28] F.J. Lin and R.J. Wai, Hybrid control using recurrent fuzzy neural network for linear induction motor servo drive, *IEEE Trans. Fuzzy Syst.* 9 (2001) 102–115.
- [29] F. Barrero, A. Gonzalez, A. Torralba, E. Galvan, L.G. Franquelo, Speed control of induction motors using a novel fuzzy sliding-mode structure, *IEEE Trans. Fuzzy Syst.* 10 (2002) 375–383.
- [30] R.J. Wa, K.M. Lin, Robust decoupled control of direct field oriented induction motor drive. *IEEE Trans. Indust. Elec.* 52 (2005) 837–854.
- [31] H.M. Soliman, E.H.E. Bayoumi, M. Soliman, Robust guaranteed-cost sliding mode control of brushless DC motor: An LMI approach, *Int. J. Model. Ident. Control* 17 (2012) 251–260.
- [32] E.H.E. Bayoumi, Sliding mode position control of synchronous motor with parameters and load uncertainties, *Electromotion Sci. J.* 17 (2010) 99–106.
- [33] H.M. Soliman, E.H.E. Bayoumi, M. Soliman, LMI-based sliding mode control for brushless DC motor drives, *Proc. IMechE Part I: J. Syst. Control Eng.* 223 (2009) 1035–1043.
- [34] R.V. Rao, V.J. Savsani, D.P. Vakharia, Teaching–learning-based optimization: A novel method for constrained mechanical design optimization problems, *Comput. Aided Des.* 43 (2011) 303–315.
- [35] K. Ameli, R. Ghazi, A. Azemi, Adaptive fuzzy sliding-mode speed and position controllers for induction motor drives, *MSc. Thesis, Ferdowsi University of Mashhad, Mashhad, Iran*, 2002.
- [36] J.E. Slotine, W. Li, *Applied Nonlinear Control*, Prentice-Hall Englewood Cliffs, NJ, 1991.
- [37] F.I. Lin, S. L. Chiu, Adaptive fuzzy sliding-mode control for PM synchronous servo motor drives, *IEE Proc. Electr. Power Appl.* 145 (1998) 63–72

## طراحی کنترل کننده سرعت بهینه بر اساس الگوریتم بهینه‌سازی مبتنی بر آموزش و یادگیری برای موتورهای القایی با استفاده از کنترل کننده فازی مود لغزشی

علیرضا الفی

دانشیار، دانشکده مهندسی برق و رباتیک، دانشگاه صنعتی شاهرود، شاهرود، ایران، a\_alfi@shahroodut.ac.ir

چکیده- در این مقاله از الگوریتم بهینه‌سازی مبتنی بر آموزش و یادگیری (TLBO) برای کنترل سرعت موتورهای القایی با استفاده از کنترل کننده مود لغزشی استفاده می‌شود. ساختار کنترل پیشنهادی به‌عنوان یک مساله بهینه‌سازی فرموله می‌شود. ابتدا یک کنترل کننده سرعت مود لغزشی با سطح کلیدزنی انتگرالی طراحی می‌شود که در آن نیازی به اطلاعات شتاب برای کنترل سرعت نیست. در این حالت، باند بالایی عدم قطعیت‌های مجتمع شامل عدم قطعیت پارامتری و اغتشاش باری در دسترس هستند. اهمیت این پارامتر بر عملکرد سیستم نشان داده می‌شود. سپس، کنترل کننده سرعت مود لغزشی فازی برای تخمین باند بالایی عدم قطعیت‌های مجتمع طراحی می‌شود. در نهایت، الگوریتم TLBO برای تعیین بهینه باند بالایی عدم قطعیت‌های مجتمع به کار برده می‌شود. نتایج شبیه‌سازی برای بیان برتری کنترل کننده پیشنهادی در مقایسه با کنترل کننده مرسوم تناسبی-انتگرال گیر، کنترل کننده مود لغزشی، کنترل کننده فازی مود لغزشی و کنترل کننده فازی تطبیقی مود لغزشی آورده می‌شود.

واژه‌های کلیدی: موتور القایی، کنترل مود لغزشی، الگوریتم بهینه‌سازی مبتنی بر آموزش و یادگیری، کنترل فازی.